ISSN 1063-7761, Journal of Experimental and Theoretical Physics, 2015, Vol. 120, No. 6, pp. 1005–1011. © Pleiades Publishing, Inc., 2015.
Original Russian Text © V.V. Melnikov, 2015, published in Zhurnal Eksperimental'noi i Teoreticheskoi Fiziki, 2015, Vol. 147, No. 6, pp. 1162–1169.

SOLIDS AND LIQUIDS

Structural and Energy Properties of Interstitial Molecular Hydrogen in Single-Crystal Silicon

V. V. Melnikov
Tomsk State University, pr. Lenina 36, Tomsk, 634050 Russia
e-mail: melnikov@phys.tsu.ru
Received October 27, 2014

Abstract—The structural and energy characteristics of interstitial molecular hydrogen in single-crystal silicon are theoretically studied. The dependence of the potential energy of the system on the position and orientation of the interstitial defect is investigated, and the mechanism of interaction of a hydrogen molecule with a silicon crystal is considered. A three-dimensional model is employed to calculate the energy spectrum of H_2 in Si, and the obtained dispersion law is analyzed.

DOI: 10.1134/S1063776115060199

1. INTRODUCTION

Single-crystal silicon is one of the basic materials for the development and production of semiconductor devices and elements. Interstitial hydrogen substantially affects the physical and chemical properties of the material, which is significant for many technological processes [1]. Control of diffusion and the hydrogen distribution in the semiconductor bulk are important aspects for a number of technologies, e.g., such as Smart Cut [2]. A detailed investigation of the effects of presence of hydrogen in silicon and other semiconductors is a challenging problem whose solution will help to decrease the size of semiconductor elements to the nanometer scale, to develop and optimize the existing technologies, to increase the control and controllability of the characteristics of semiconductor elements, and to simulate technological processes and the properties of materials.

An analysis of the available results of experimental and theoretical investigations of the H_2–Si system (see, e.g., [1–20] and Refs. therein) leads to the following conclusions. Atomic hydrogen penetrates into the structure of the semiconductor at almost all stages of technological processes. Some of embedded atoms form molecular hydrogen [3–6]. An H_2 molecule strongly interacts with a silicon matrix, which significantly increases the H–H bond length and decreases the vibrational frequencies [7–11]. In addition, H_2 exhibits the properties of a free rotator; that is, rotational degrees of freedom are not "frozen," and the spectra of the interstitial defect can be interpreted using the free molecule model [12–19]. In an equilibrium configuration, the center of mass of H_2 is located at the tetrahedral site (T site) of the Si crystal lattice, and the molecule is oriented along directions equivalent to [100] with a rotational potential barrier of about 0.01 eV [13, 19]. According to [20] (where the kinetics of O–H complexes in crystalline silicon was considered), the activation energy of diffusion of molecular hydrogen is about 0.78 eV.

The purpose of this work is to study the structural and energy characteristics of interstitial molecular hydrogen in single-crystal silicon in terms of ab initio calculations. We analyzed the energy of the system as a function of the position of an interstitial defect, calculated the minimum energy path (MEP) between the equilibrium hydrogen sites in a crystal with allowance for the rotational degree of freedoms of the molecule, estimated the response of the silicon matrix to the presence of H_2, and considered the mechanism of interaction of the molecule with the crystal. Since hydrogen is the lightest molecule and is placed in the periodic potential of crystalline silicon, we calculated the energy spectrum of H_2 in the 3D potential of the silicon matrix.

2. COMPUTATIONAL METHOD

The atomic and electronic structures of the H_2–Si system were calculated using the density functional theory with the PW91 exchange-correlation functional [21] in the generalized gradient approximation [22, 23] implemented in the CRYSTAL09 software package [24].

The system was considered within the framework of the cubic supercell model with periodic boundary conditions. The cell size was chosen so that the interaction of hydrogen molecule with its periodic images was excluded. In the calculations, we used superlattices consisting of 4 and 32 primitive cells of crystalline silicon, i.e., the structures consisting of 8 and 64 silicon atoms, respectively. Massive calculations were mainly performed on the smaller cell, and the calcula-

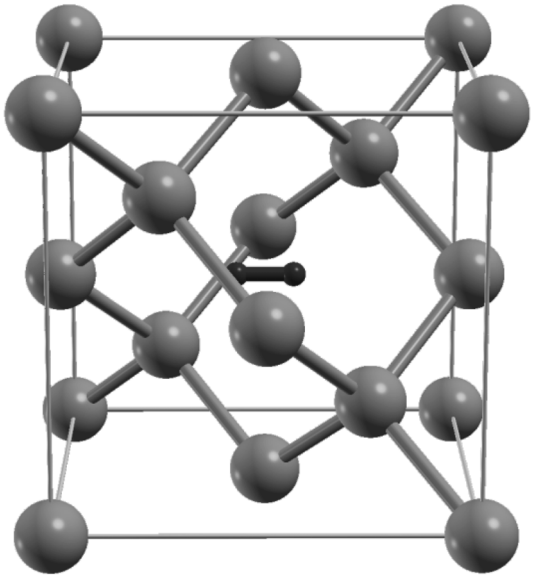

Fig. 1. Calculation supercell with a hydrogen molecule at the *T* site.

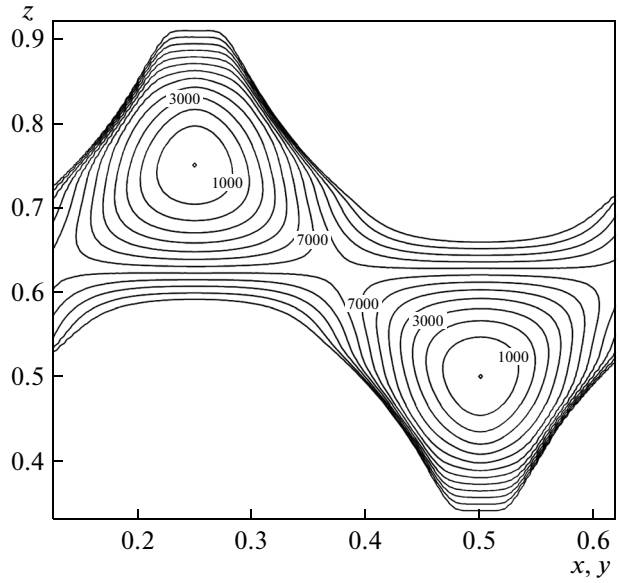

Fig. 2. Potential energy of the interaction of a hydrogen molecule with crystalline silicon in the $(\bar{1}10)$ plane. Isoenergetic contours are plotted at a step of 1000 cm^{-1}.

tions carried out for certain atomic configurations were repeated on the larger cell to control the obtained results and to study critical cases.

Figure 1 shows the small supercell. In calculations of the potential energy of the hydrogen molecule in of the single-crystal silicon, the Si atoms were fixed at their equilibrium positions of the ideal crystal. The energy of the system was analyzed for a large number of possible H_2 sites in the cell. Ab initio calculations were performed using an $8 \times 8 \times 8$ grid of *k*-points for the small cell and a $4 \times 4 \times 4$ grid for the large one. Based on analysis of the results of solution of the electronic problem for the model structure and reproduction of various properties, we choose the optimized Si basis set from [25] and the Dunning DZP basis set for the hydrogen atoms [26]. Since the localized basis functions were used, the basis set superposition error (BSSE) correction was always taken into account.

The calculated lattice parameter of silicon (a = 5.47 Å) differs from the experimental parameter (a = 5.43 Å) by at most 0.7%. The bond length in H_2 was calculated to be 0.7487 Å (which is slightly larger than the experimental bond length (0.7414 Å) [27]) for the free molecule and 0.7810 Å for hydrogen in the silicon crystal. The last value was used in the ab intio calculations of the energy of the system for various hydrogen molecule positions in the single crystal.

According to the adiabatic approximation, the obtained ab initio values of system energy E were used as the potential energy of a hydrogen molecule in the silicon single crystal $V(x, y, z, \theta, \varphi)$, where θ and φ are the spherical coordinates with the origin at the center of mass of the molecule and x, y, and z are the coordinates of the center of mass of H_2 in the crystal cell. The Cartesian coordinate system was chosen so that the directions of its basis vectors coincided with the calculation cell vector directions. The zero value of angle θ corresponds to the molecule orientation along axis z. For example, the center of mass of an H_2 molecule in Fig. 1 is located at the point (1/2, 1/2, 1/2), $\theta = 90°$, $\varphi = 0°$.

When calculating the energy states of H_2 in Si, we took into account only translational degrees of freedoms. The three-dimensional periodic potential of interaction of the molecule with the crystal was represented by the ab initio system energies for various H_2 sites in the cell averaged over the angular variables.

The corresponding stationary Schrödinger equation with periodic boundary conditions was numerically solved using a variational approach. The Bloch wavefunctions were represented in the form of plane wave expansion, and the matrix elements of the system Hamiltonian were calculated using the discrete Fourier transform. The energy levels of the interstitial defect $\varepsilon(\mathbf{k})$ were calculated for the values of wavevector $\mathbf{k}$ that fall in segments L–Γ–X/X'–K–Γ. In this case, the primitive cell of silicon was used as the element of a periodic structure. The uniformly distributed calculation grid contained $54 \times 54 \times 54$ points, and the cutoff energy for plane wave basis set was 16000 cm^{-1}, which allowed to ensure good convergence of the eigenvalues in the considered range of the energy

Energy and structural characteristics for the equilibrium and transition positions of a hydrogen molecule in a silicon crystal

	θ, deg	φ, deg	Value for fixed structure, cm^{-1}	Change after relaxation, cm^{-1}	Average shift of the nearest Si atoms, Å
E_{eq}	90	0	0	−145	0.02
$\min E_{sp}$	129.1	45	7961	−881	0.04
$\max E_{sp}$	54.7	45	8947	−916	0.04

spectrum. The solution algorithm was implemented in the form of FORTRAN program.

3. RESULTS AND DISCUSSION

Figure 2 shows the potential energy of interaction of a hydrogen molecule with crystalline silicon in the $(\bar{1}10)$ plane averaged over the rotational variables. The minima at the points (1/2, 1/2, 1/2) and (1/4, 1/4, 3/4) correspond to the equilibrium positions of the molecule in the matrix, i.e., two neighboring T sites. The potential barrier between these minima—a saddle point with the coordinates (3/8, 3/8, 5/8)—is about 1 eV. The step for the drawn isoenergetic contours is 1000 cm^{-1}, and the constant-energy contours located at the maximum distance from the minima correspond to an energy of 12 000 cm^{-1}. The calculated energies that were higher than this energy were not used to plot these curves because of high potential gradients.

To estimate the influence of interstitial molecular hydrogen on the internal crystal geometry and the corresponding system energy, we optimized the structure of Si with H_2 fixed in the following positions: the equilibrium, the saddle point with two molecule orientations corresponding to the minimum ($\min E_{sp}$) and the maximum ($\max E_{sp}$) system energies, as well as along the MEP. The response of the structure to introduction of the molecule is illustrated by the data in the table. The calculations showed that system energy E_{eq} for the T site decreases by approximately 145 cm^{-1} as a result of restructuring of the nearest environment of H_2: four neighboring Si atoms are displaced from the molecule by about 0.2 Å. The crystal structure undergoes more notable changes at the saddle point, where the distance from H_2 to the nearest silicon atoms decreases. However, the maximum rotational barrier in this position, i.e., $\max E_{sp} - \min E_{sp}$, changes insignificantly during structural optimization and is about 10^3 cm^{-1}.

Figure 3 shows the MEP of a hydrogen molecule between the neighboring equilibrium positions. Hereafter, for definition, we consider T sites with the coordinates (1/2, 1/2, 1/2) and (3/4, 3/4, 3/4) and the saddle point (5/8, 5/8, 5/8). According to the structure and symmetry of the system, all possible MEPs lie in {110} planes. One can see that the difference between the potential energies of the system along the MEPs obtained without and with allowance for silicon atom relaxation changes in the range 10^2–10^3 cm^{-1} and

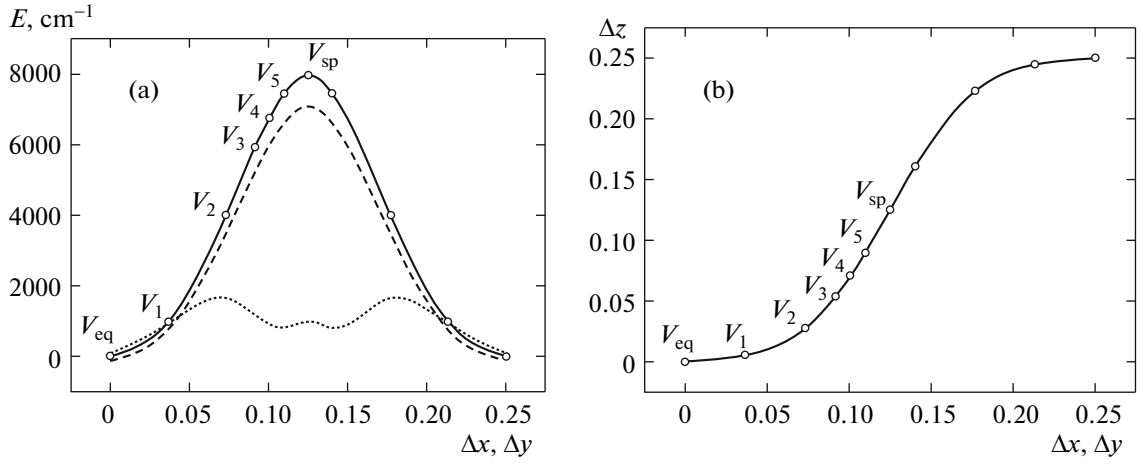

Fig. 3. The minimum energy path of H_2 molecule between the neighboring equilibrium positions in a silicon crystal. (a): (solid curve) potential barrier for the fixed structure of Si, (dashed curve) potential barrier after structural optimization, and (dotted curve) difference between $\max E$ and $\min E$ at the point with displacement (Δx, Δy, Δz) relative to the equilibrium site. (b) The corresponding molecule motion trajectory.

increases monotonically when saddle point V_{sp} is approached. The maximum rotational barrier increases when the molecule goes from point V_{eq} to point V_2 and reaches an extreme value of ~1600 cm^{-1} in the vicinity of this point. Then, in the range V_2–V_5, the difference between max$E$ and min$E$ decreases to about 800 cm^{-1}. At transition point V_{sp}, the system energy increases by about 100 cm^{-1}. The average difference max$E$ – min$E$ calculated along the entire path is about 900 cm^{-1}. It should be noted that MEP degenerates into the straight line coinciding with a [111] diagonal when the potential energy of the system is averaged over the rotational variables.

Figure 4 shows the potential energy of the system as a function of the molecule orientation along MEP. The magnitude of the radius vector of a point on the displayed surfaces is $V(x, y, z, \theta, \varphi)$ minus the minimum energy for the corresponding fixed position of the center of mass of H_2 molecule in MEP (see Fig. 3). From a classical standpoint, this angular dependence of energy can be interpreted as the appearance of a preferred axis of hydrogen molecule rotation, and the classical axis of rotation is predominantly oriented along the $[11\bar{1}]$ direction in the MEP segment V_1–V_3 (Figs. 4b, 4c). Approximately on the segment V_3–V_5, the orientation of the assumed axis of rotation changes (Figs. 4c–4e), and the axis is oriented along a [111] direction in the segment V_5–V_{sp} (Figs. 4e, 4f). It is also interesting that the maximum system energy corresponds to the position of the molecule along a [111] direction at transition point V_{sp}. Thus, the molecule is mainly directed parallel to the (111) plane during the passage through the potential barrier, which is not an obvious consequence of the structure geometry and becomes clear only when the interaction of H_2 with Si is considered on a microlevel.

The mechanism of interaction of the molecule with the crystal was analyzed using the ab initio calculated spatial distribution of charge density difference $\Delta\rho(\mathbf{r})$,

$$\Delta\rho(\mathbf{r}) = \rho_{H_2}(\mathbf{r}) + \rho_{Si}(\mathbf{r}) - \rho_{H_2/Si}(\mathbf{r}), \quad (1)$$

where ρ_{H_2} and ρ_{Si} are the charge densities of the isolated molecule and the crystal, respectively, and $\rho_{H_2/Si}$ is the total charge density of the H_2–Si system. The presence of regions with negative/positive values of $\Delta\rho(\mathbf{r})$ points to an increase/decrease in the electron density in the crystal volume when the molecule is introduced. As an example, Fig. 5 shows $\Delta\rho(\mathbf{r})$ distributions for the following two hydrogen molecule positions: at the T site and at the saddle point with the bond orientation along [111] direction. These isosurfaces are the boundaries of the regions where the electron density is mainly redistributed.

In the case of the equilibrium position of H_2 molecule, the charge redistribution induced by its interaction with Si atoms is mainly localized in the vicinity of the introduced molecule (Fig. 5a). Here, the electron density near hydrogen atoms increases, and a toroidal region with positive values of $\Delta\rho$ arises around the molecule axis. This charge redistribution indicates a significant role of ionic and polarization interactions. $\Delta\rho$ distributions with a similar topology and localization are also observed when the molecule are displaced from the T site at a distance up to 0.3 Å. For larger displacements (with the corresponding decrease in the distance between H_2 and some of the nearest Si atoms), less localized changes in the electronic structure are observed.

Along MEP, the involvement of crystalline silicon in the formation of interatomic bonds is maximal at transition point V_{sp} when a hydrogen molecule is oriented along a [111] direction (Fig. 5b), i.e., at the position where the system energy is maximal (maxE_{sp}). At this point, together with negative $\Delta\rho$ regions near hydrogen atoms and a positive toroidal region, a "hexagonal belt" of negative values of $\Delta\rho$ passing through six nearest silicon atoms arises here. We could assume that the presence of such a closed region with a high charge carrier density can cause the formation of collective quasi-bound electronic states with a nonzero momentum (or ring microcurrents from a classical standpoint) under certain conditions. However, taking into account the dynamics and energetics of the processes occurring in the crystal, it is reasonable to assume that the probability of appearance of such states should remain extremely low.

The specific features of the band structure of the energy levels of a hydrogen molecule in a silicon crystal that were revealed in the study of a two-dimensional model of the system [28] manifest themselves to a great extent in the spectrum of H_2 calculated for a three-dimensional potential. According to the system symmetry, the lower energy levels are degenerate, and additional twofold degeneracy at fixed values of wavevector $\mathbf{k}$ appears due to the existence of two equivalent equilibrium sites for H_2 molecule in the unit cell of silicon. As the energy increases, the probability of tunneling transition of the molecule between the T sites increases, and a band structure formation takes place.

According to the calculations, the weak splitting of the energy levels of H_2 that results in a band formation with the width $\Delta \approx 0.1$ cm^{-1} arises for energies of about 6000 cm^{-1} (hereafter, all energies are given relative to the ground state $E_0 \approx 1102.2$ cm^{-1}). The last value exceeds the corresponding energy obtained for the two-dimensional model by approximately 35 cm^{-1}. Bands with $\Delta \approx 0.6$ cm^{-1} are formed in the range 6603–6606 cm^{-1} (Fig. 6a). Bands about 7 cm^{-1} wide are observed for energies

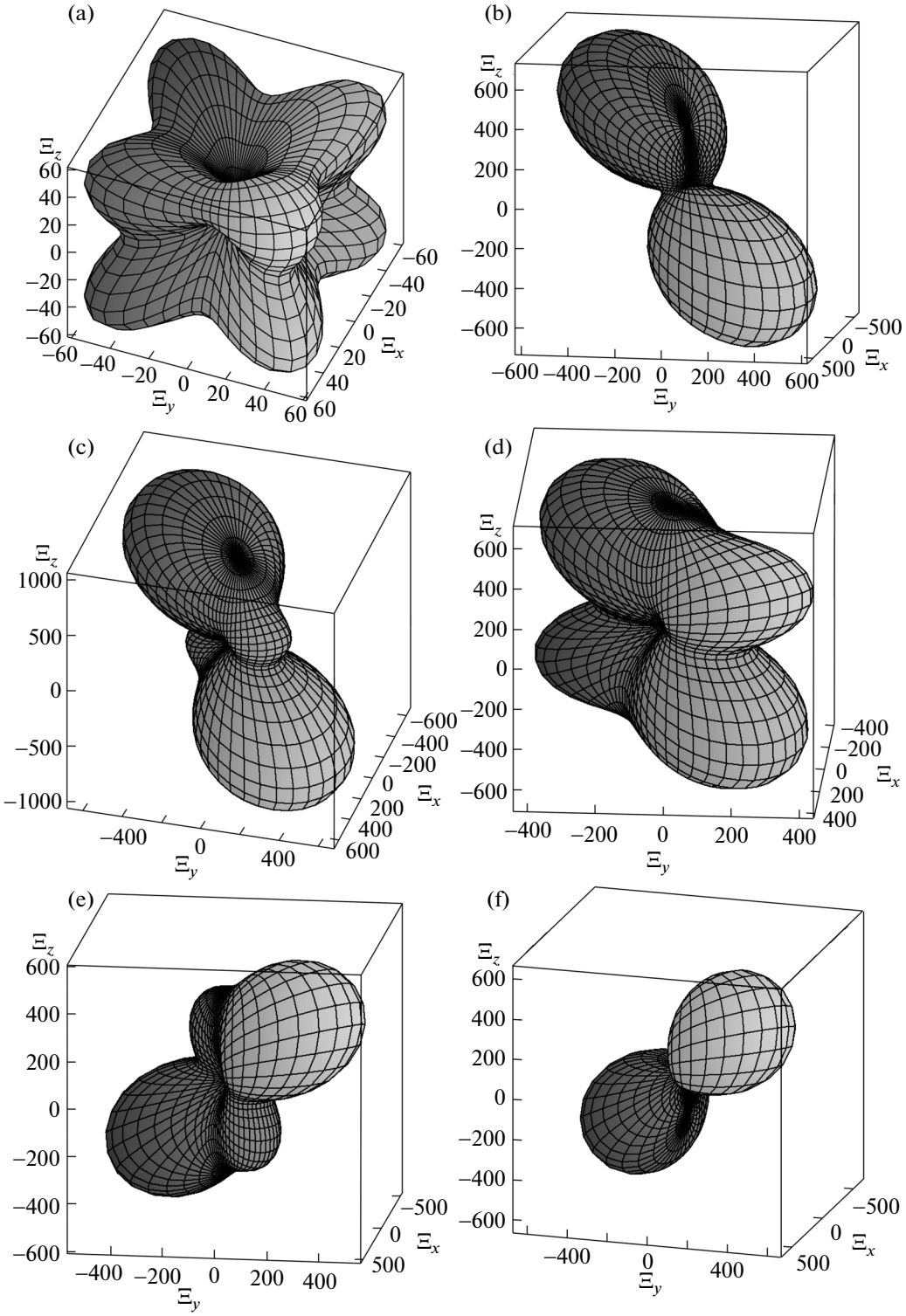

Fig. 4. Potential energy (cm^{-1}) of the system vs. the orientation of a hydrogen molecule. The direction of radius vector Ξ of the point on the displayed surfaces is determined by angles θ and ϕ, and its magnitude is equal to the values of the differences $E - \min E$ that correspond to different positions of the center of mass of the H_2 molecule in MEP (see Fig. 3): (a) equilibrium position, V_{eq}; (b) V_1; (c) V_3; (d) V_4; (e) V_5; and (f) saddle point, V_{sp}.

of 7600 and 7970 cm^{-1}. Figure 6b shows the structure of energy levels in the range 8030–8080 cm^{-1}, where we have $\Delta \approx 12$ cm^{-1} and $\Delta \approx 19$ cm^{-1} for two bands. Note that the $\varepsilon(\mathbf{k})$ dispersion laws in the segment $X'-L-\Gamma$ that were obtained in this work and [28] agree qualitatively with each other.

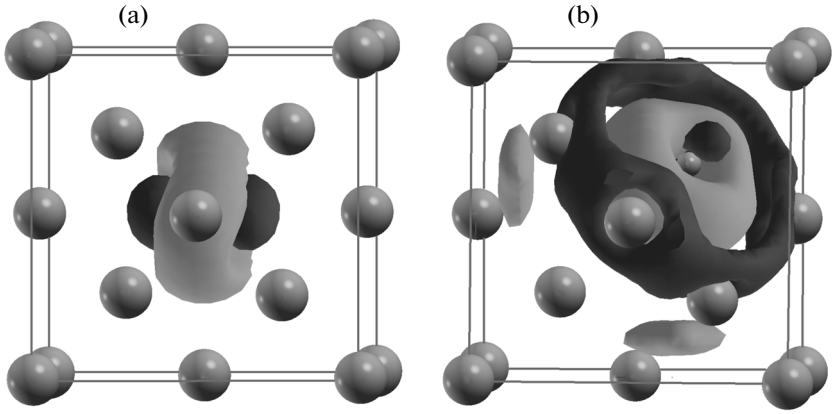

Fig. 5. Distribution of charge density difference Δρ: (a) hydrogen molecule at the T position and (b) H_2 is located at saddle point V_{sp} with the bond oriented along a [111] direction. Bright and dark regions correspond to positive and negative values of Δρ.

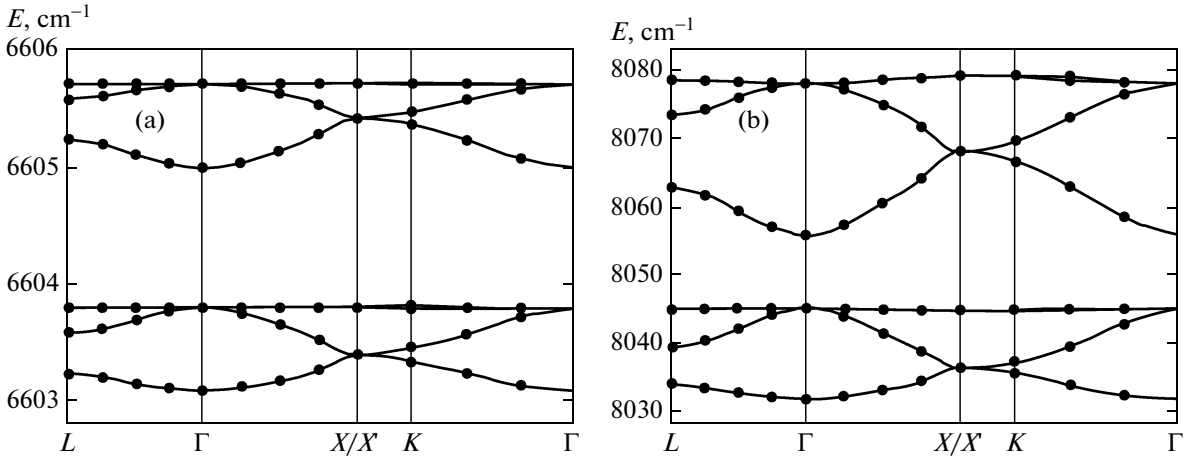

Fig. 6. Band structure of the energy levels of H_2 in a Si crystal.

An analysis of the group velocity of the molecule on the wavevector direction shows that this velocity is maximal for directions equivalent to [100] and is minimal for directions equivalent to [111]. This result agrees with the observation of hydrogen-containing planar defects (platelets), which are formed predominantly in {111} planes [1]. Although a vacancy mechanism is considered to play a key role in the formation of such defects, this orientation remains predominant even in terms of the ideal crystal model.

4. CONCLUSIONS

Ab initio calculations of the atomic and electronic structures of interstitial molecular hydrogen in single-crystal silicon were carried out. The potential energy of the system was analyzed as a function of the position and orientation of the interstitial defect, and the mechanism of molecule–crystal interaction was considered. The MEP of H_2 molecule between T positions in silicon was calculated with allowance for the rotational degrees of freedom and the response of the crystal structure. According to the calculation results, the minimum and maximum energy barriers E_{sp} for the fixed structure of Si are approximately 7961 and 8947 cm^{-1}. When structural relaxation was taken into account, these values decreased by about 1000 cm^{-1}, approaching the experimental value (0.78 eV). The maximum energy of the system at a saddle point was found to be reached when a hydrogen molecule is oriented along [111] direction.

Within the framework of the model proposed here, the energy spectrum of H_2 in the three-dimensional potential of the silicon matrix was calculated. It was found that a band structure is formed at the energies that exceed the ground state of the defect ($E_0 \approx$ 1102.2 cm^{-1}) approximately by 6000 cm^{-1}. The calculated dispersion law agrees with the occurrence of

hydrogen-containing planar defects, which are mainly formed in {111} planes.

ACKNOWLEDGMENTS

The numerical calculations were performed on the SKIF Cyberia supercomputer and were supported by the Regional Center for Collective Use of High-Performance Computational Resources of Tomsk State University.

This work was supported by the Ministry of Education and Science of the Russian Federation, project no. 2014/223, code 727.

REFERENCES

1. S. J. Pearton, J. W. Corbett, and M. Stavola, *Hydrogen in Crystalline Semiconductors* (Springer-Verlag, Berlin, 1992).
2. M. Bruel, Electron. Lett. **31**, 1201 (1995).
3. A. W. R. Leitch, V. Alex, and J. Weber, Phys. Rev. Lett. **81**, 421 (1998).
4. A. Mainwood and A. M. Stoneham, Physica B (Amsterdam) **116**, 101 (1983).
5. J. W. Corbett, S. N. Sahu, T. S. Shi, and L. C. Snyder, Phys. Lett. A **93**, 303 (1983).
6. S. K. Estreicher, Mater. Sci. Eng., R **14**, 319 (1995).
7. Y. Okamoto, M. Saito, and A. Oshiyama, Phys. Rev. B: Condens. Matter **56**, 10016 (1997).
8. K. G. Nakamura, K. Ishioka, M. Kitajima, N. Fukata, K. Murakami, A. Endou, M. Kubo, and A. Miyamoto, Appl. Surf. Sci. **130**, 243 (1998).
9. B. Hourahine, R. Jones, S. Oberg, R. C. Newman, P. R. Briddon, and E. Roduner, Phys. Rev. B: Condens. Matter **57**, 12666 (1998).
10. C. G. Van de Walle and J. P. Goss, Mater. Sci. Eng., B **58**, 17 (1999).
11. Yong-Sung Kim, Young-Gu Jin, Ji-Wook Jeong, and K. J. Chang, Physica B (Amsterdam) **273**, 231 (1999).
12. S. K. Estreicher, J. L. McAfee, P. A. Fedders, J. M. Pruneda, and P. Ordejo'n, Physica B (Amsterdam) **308**, 202 (2001).
13. W. B. Fowler, P. Walters, and M. Stavola, Phys. Rev. B: Condens. Matter **66**, 075216 (2002).
14. E. V. Lavrov and J. Weber, Phys. Rev. Lett. **89,** 215501 (2002).
15. M. Hiller, E. V. Lavrov, and J. Weber, Phys. Rev. B: Condens. Matter **74**, 235214 (2006).
16. M. Hiller, E. V. Lavrov, and J. Weber, Phys. Rev. Lett. **98**, 055504 (2007).
17. J. Weber, M. Hiller, and E. V. Lavrov, Physica B (Amsterdam) **401**, 91 (2007).
18. C. Peng, M. Stavola, W. B. Fowler, and M. Lockwood, Phys. Rev. B: Condens. Matter **80**, 125207 (2009).
19. V. V. Melnikov and S. N. Yurchenko, Russ. Phys. J. **56** (12), 1363 (2013).
20. V. P. Markevich and M. Suezawa, J. Appl. Phys. **83**, 2988 (1998).
21. J. P. Perdew, J. A. Chevary, S. H. Vosko, K. A. Jackson, M. R. Pederson, D. J. Singh, and C. Fiolhais, Phys. Rev. B: Condens. Matter **48**, 4978 (1993).
22. J. P. Perdew and Y. Wang, Phys. Rev. B: Condens. Matter **33**, 8800 (1986).
23. J. P. Perdew, Phys. Rev. B: Condens. Matter **33**, 8822 (1986).
24. R. Dovesi, R. Orlando, B. Civalleri, C. Roetti, V. R. Saunders, and C. M. Zicovich-Wilson, Z. Kristallogr. **220**, 571 (2005); R. Dovesi, V. R. Saunders, C. Roetti, R. Orlando, C. M. Zicovich-Wilson, F. Pascale, B. Civalleri, K. Doll, N. M. Harrison, I. J. Bush, P. D'Arco, and M. Llunell, *CRYSTAL09 User's Manual* (University of Torino, Torino, Italy, 2009).
25. F. J. Torres, B. Civalleri, C. Pisani, and P. Ugliengo, J. Phys. Chem. B **110**, 10467 (2006).
26. T. H. Dunning, Jr., J. Chem. Phys. **53**, 2823 (1970).
27. A. P. Babichev, N. A. Babushkina, A. M. Bratkovskii, et al., in *Handbook of Physical Quantities*, Ed. by I. S. Grigoriev and E. Z. Meilikhov (Energoatomizdat, Moscow, 1991; CRC Press, Boca Raton, Florida, Unites States, 1996).
28. V. V. Melnikov, Russ. Phys. J. **57** (9), 1294 (2014).

Translated by K. Shakhlevich